Electroweak Corrections to gg → $\gamma\gamma$

Gabriele Fiore

In collaboration with *Ciaran Williams*

Based on: arXiv:2306.03956 and arXiv:2510.21643

ETH zürich Institute for Theoretical Physics

Motivation: Diphoton channel

- Diphoton channel has a historical importance in the discovery of the Higgs boson.

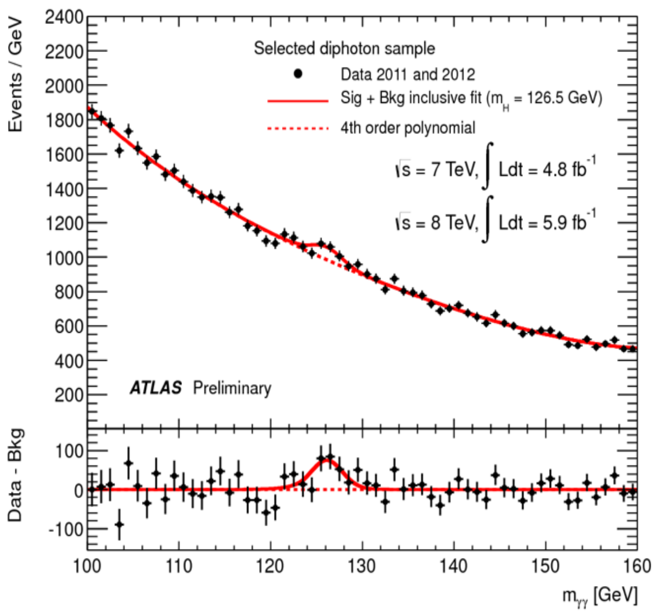

ATLAS Collaboration, 2012

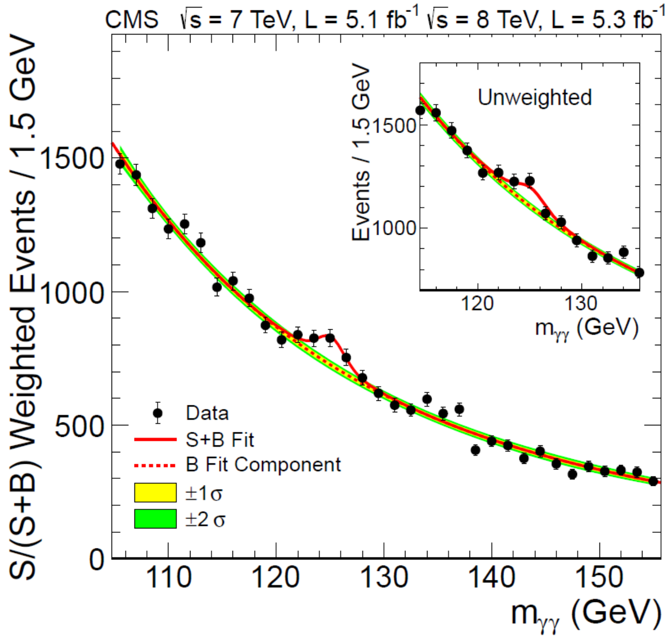

CMS Collaboration, 2012

- We distinguish between two different initial states: $q\bar{q} \to \gamma\gamma$ and $gg \to \gamma\gamma$.

Diphoton Predictions: $q\bar{q}$ Channel

$$q\bar{q} \to \gamma\gamma$$

Full NLO:

- *Binoth, Guillet, Pilon, Werlen, '99*

NNLO, QCD:

- *Catani, Cieri, de Florian, Ferrera, Grazzini, 2011*
- *Campbell, Ellis, Li, Williams, 2016*
- *Gehrmann, Glover, Huss, Whitehead, 2020*

NNLO, q_t-resummed:

- NNLL: *Cieri, Coradeschi, de Florian, 2015*
- N3LL: *Neumann, 2021*

NNLLO + NNLO_{QCD}+ PS:

- *Alioli, Broggio, Gavardi, et. al 2021*
- *Gavardi, Oleari, Re, 2022*

NNLO, top-mass effects:

- *Becchetti, Bonciani, Cieri, Coro, Ripani, 2024*

N3LO amplitude:

- *Caola, Manteuffel, Tancredi, 2020*

NLO EW corrections:

- *Bierweiler, Kasprzik, Kühn, 2013*
- +2j: *Chiesa, Greiner, Schonherr, Tramontano, 2017*

NLO QCD + jets:

- *Del Duca, Maltoni, Nagy, Trocsanyi, 2003*
- *Gehrmann, Greiner, Heinrich, 2013*
- *Badger, Guffanti, Yundin, 2013*
- *Bern, Dixon, Cordero, Hoeche, Ita, Kosower, Lo Presti, Maitre, 2014*

Diphoton Predictions: gg Channel

$$gg \to \gamma\gamma$$

NNLO:

- *Dicus, Willenbrock, '88*

N3LO, QCD:

- Ligh quarks: *Bern, Dixon, Schmidt 2002*
- Heavy quarks: *Maltoni, Mandal, Zhao, 2018*
  Chen, Heinrich, et al., 2020
  Ahmed, Chakraborty, Chaubey, Kaur, 2025
  Davies, Grau, Schönwald, Steinhauser, Stremmer, Vitti, 2025

N3LO + jet, QCD corrections:

- *Badger, Gehrmann, Marcoli, Moodie, 2021*

N4LO, QCD amplitude:

- *Bargiela, Caola, Manteuffel, Tancredi, 2022*

<u>EW corrections missing</u>

↑

Objective of today's talk!

- ➢Modern analysis, NNLO + PS matching in QCD compared with Atlas data.

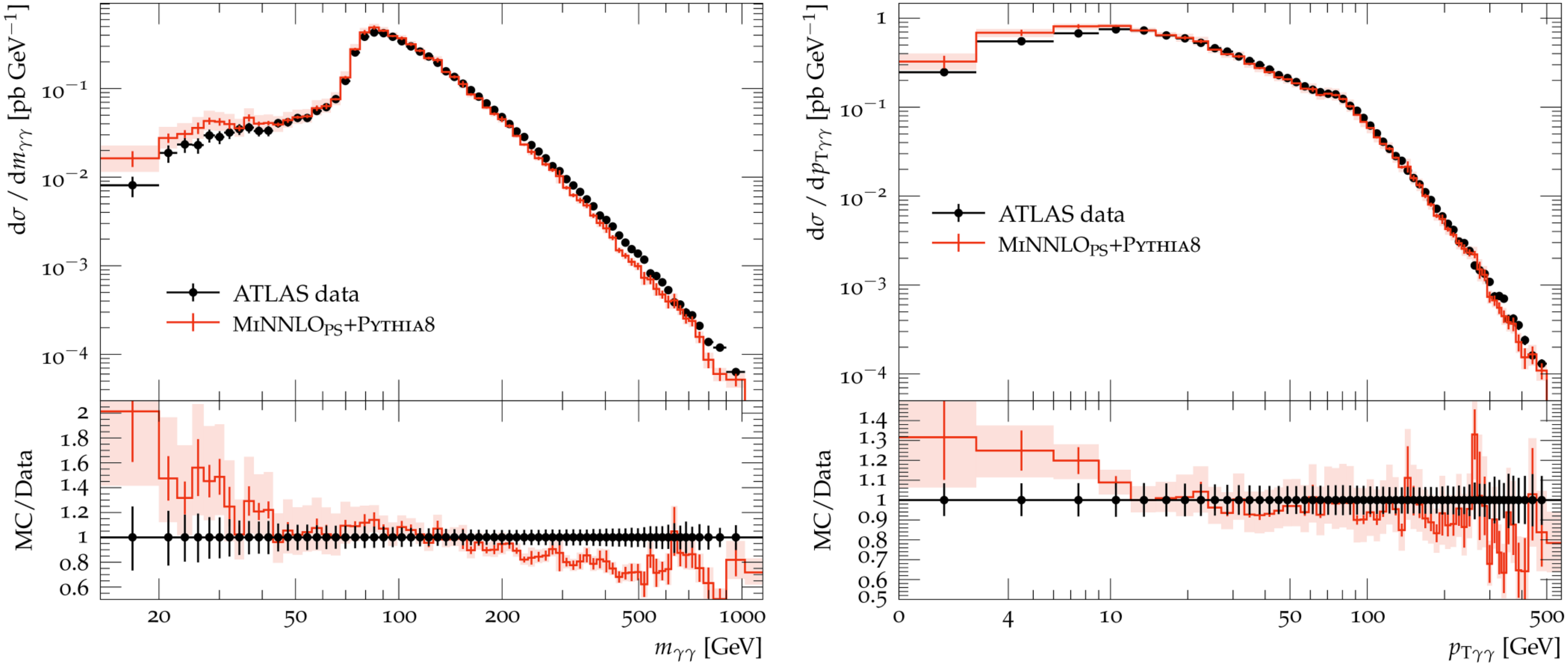

Gavardi, Oleari, Re, 2022

Diphoton Predictions: Impact of EW corrections

- With the QCD corrections reaching very high precision, the EW sector becomes more relevant.

- At high energy the Sudakov effects improve the comparison with the data.

- Similar trend is observed on different processes as well. e.g. DY with mixed QCD-EW(*Balossini, Calame, Montagna, Moretti, Nicrosini, Piccinini, Treccani, Vicini, 2009*) .

Inclusive photon production at NNLO

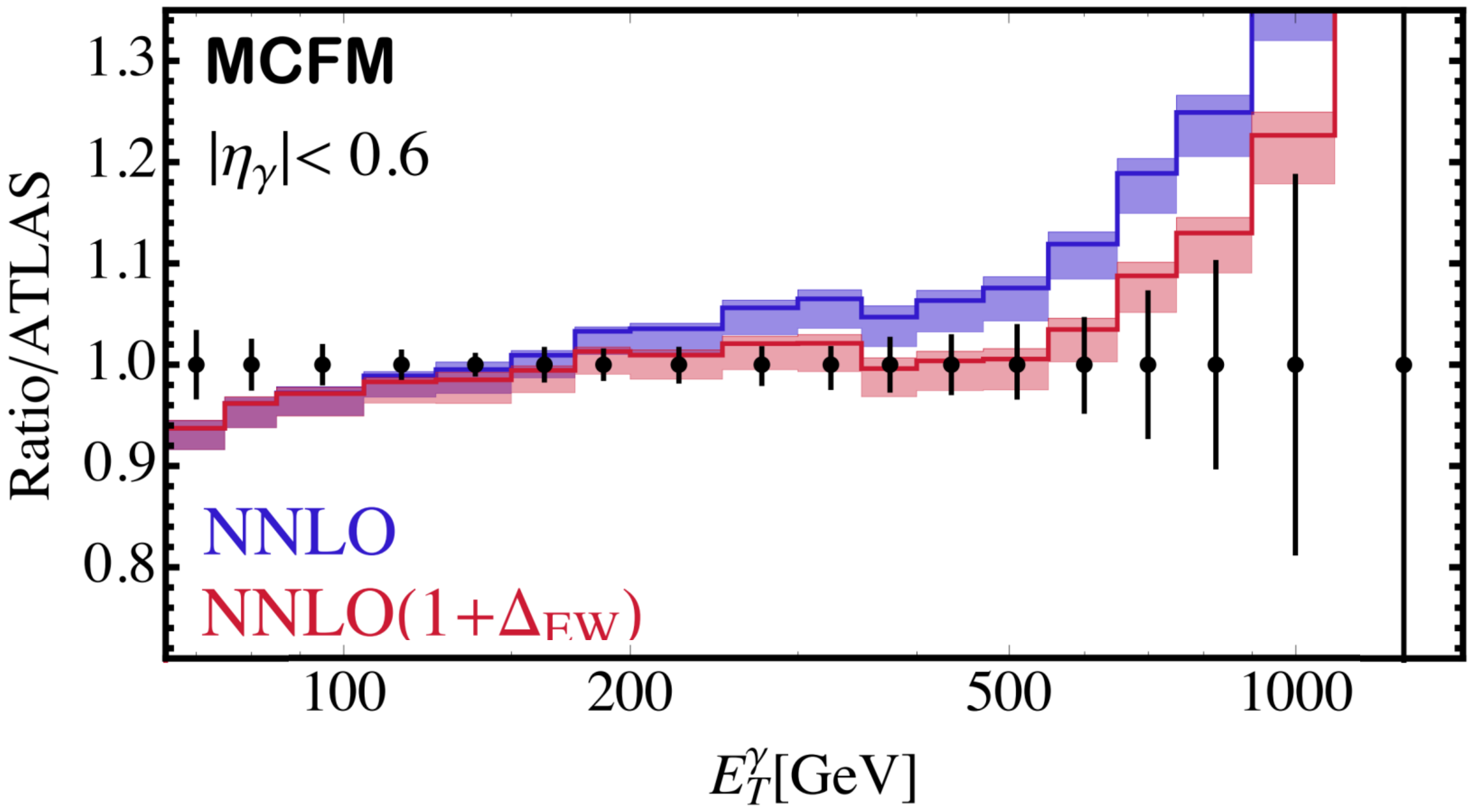

Campbell, Ellis, Williams, 2016

Motivation: gg Channel

- As part of the partonic process $pp \to \gamma\gamma$, the corrections enter at NNLO in QCD.

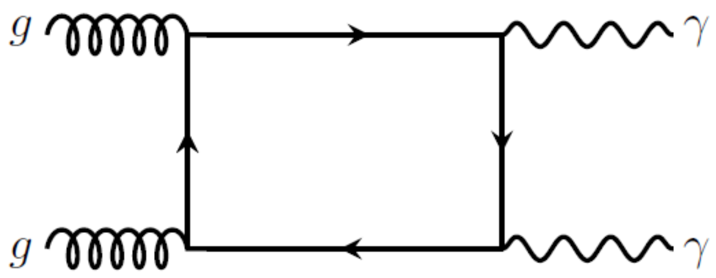

- Sizable contributions to the cross-section due to large initial-state gluon flux.
- Given the quality of recent LHC data, $\mathcal{O}(\alpha)$ corrections for the $gg \to \gamma\gamma$ channel are required to improve the precision our theoretical predictions.

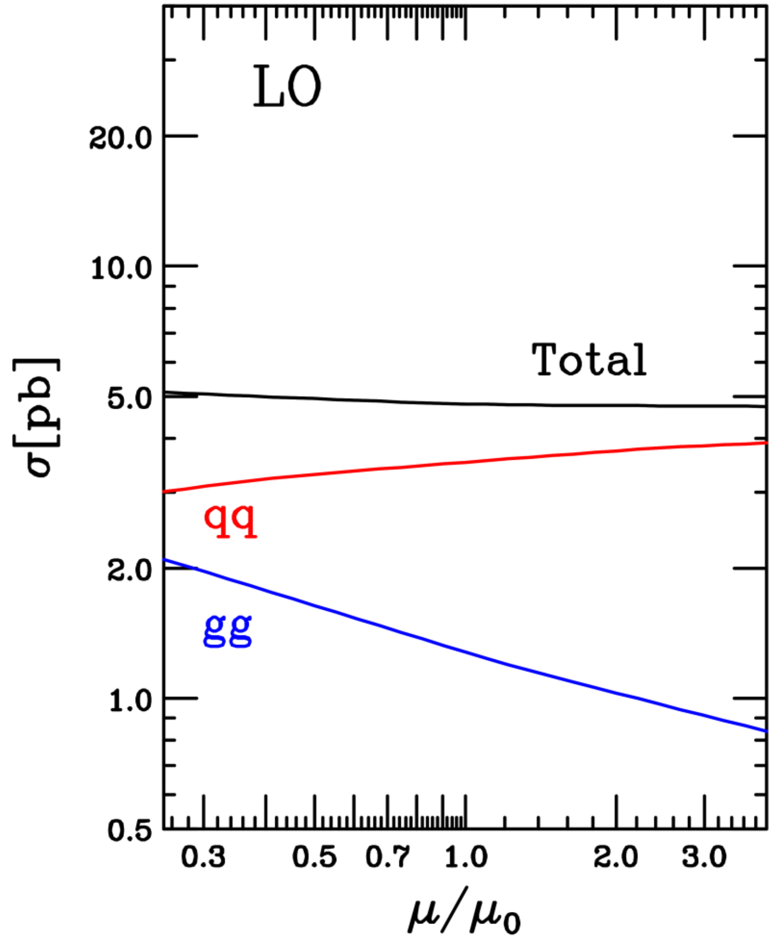

Campbell, Ellis, Williams, 2011

Motivation: gg Channel

- Below, the impact of the gg channel in the NNLO implementation of pp → γγ in MCFM. Data points taken from CMS(1405.7225).

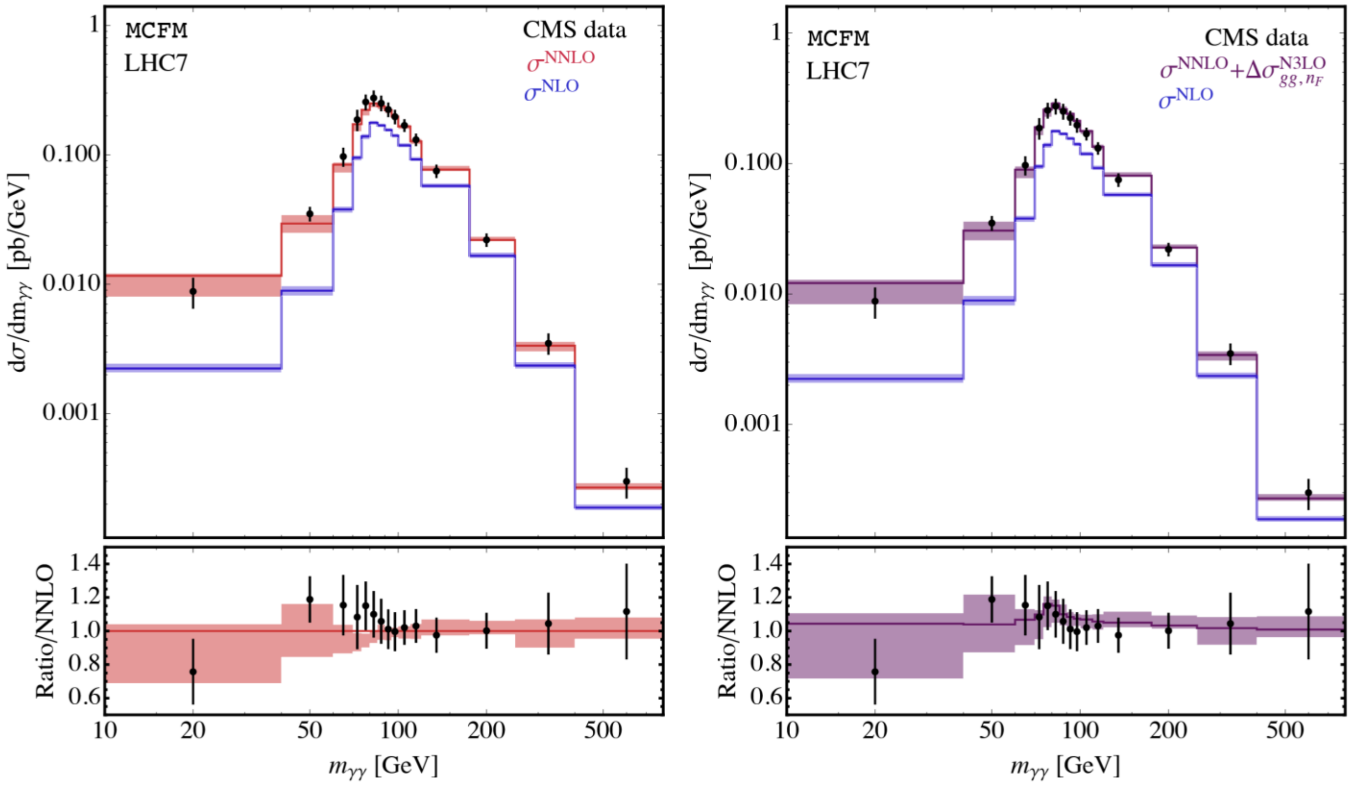

Campbell, Ellis, Li, Williams, 2016

Motivation: Interference

- $gg \to \gamma\gamma$ channel is crucial for studying the Higgs properties. A crucial example is the width, too small to be directly measured at LHC.

- The interference between the diphoton channel $gg \to H \to \gamma\gamma$ and the QCD background $gg \to \gamma\gamma$ can be used to extract better bounds on Higgs width(*Dixon, Siu, 2006; Martin, 2012; Dixon, Li, 2013*).

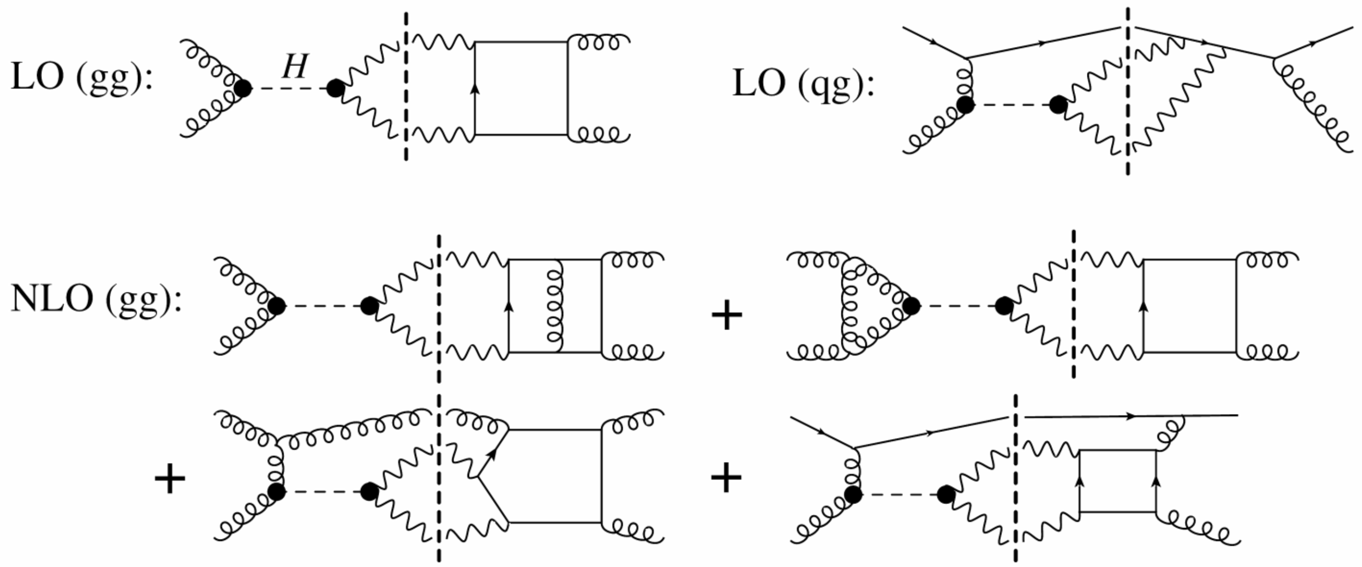

Motivation: Interference

- NLO analysis shows mass shift effect of ~ 70MeV and destructive interference to the total cross-section of about 2% at NLO in QCD(Campbell, Carena, Harnik, Liu, 2017).

- Higgs width bounded to 20-40 Γ_H^{SM}.

- These NLO QCD corrections are responsible for 40% effect on the mass shift, highlighting the relevance of higher order corrections.

- Beyond NLO (soft virtual approximation): reduction of the cross-section of about 1.7%, and an additional 30% for the mass shift on top of the NLO prediction (Bargiela, Buccioni, Caola, Devoto, Manteuffel, Tancredi, 2022).

- The EW corrections are still a missing piece in this picture!

Calculation Workflow

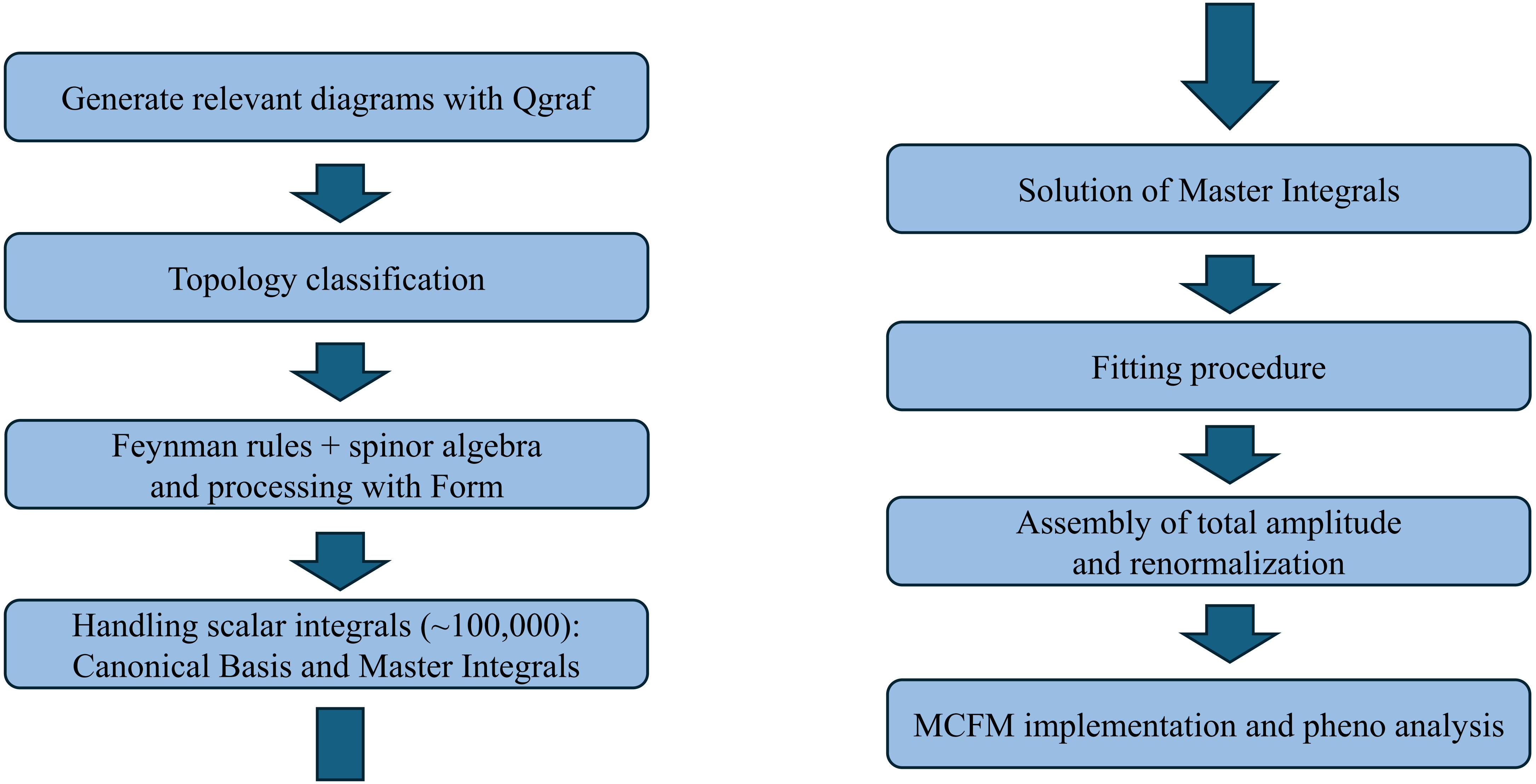

Calculation Workflow

1. Generate relevant diagrams with Qgraf
2. Topology classification
3. Feynman rules + spinor algebra and processing with Form
4. Handling scalar integrals (~100,000): Canonical Basis and Master Integrals
5. Solution of Master Integrals
6. Fitting procedure
7. Assembly of total amplitude and renormalization
8. MCFM implementation and pheno analysis

Relevant Diagrams

- Many of those are zero for the massless case (Furry theorem, charge conservation, massless limit,…).

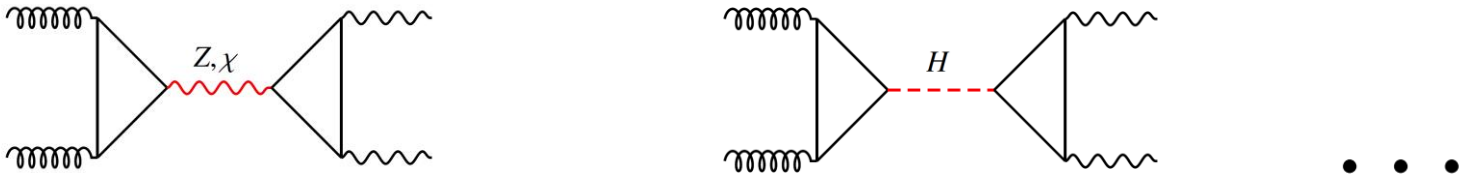

- QED diagrams already known. Use them as benchmark! (Bern, De Freitas, Dixon, 2001)

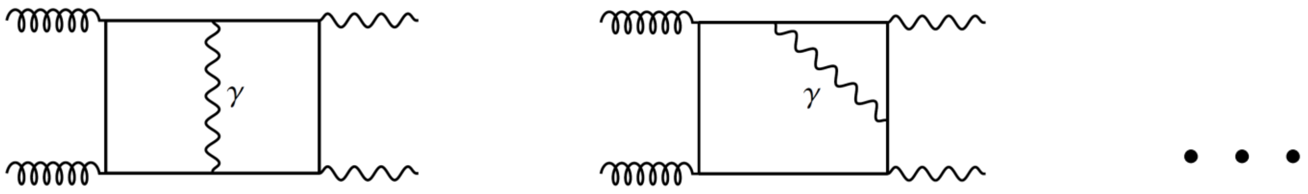

- New: pure non-abelian contributions with W-type insertion. Different behavior and charge structure.

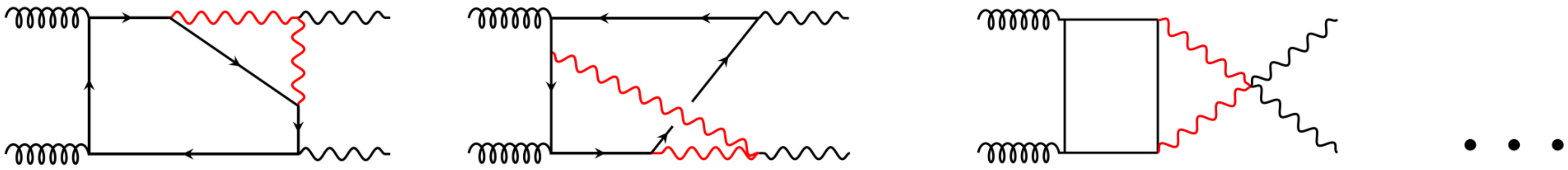

Calculation Workflow

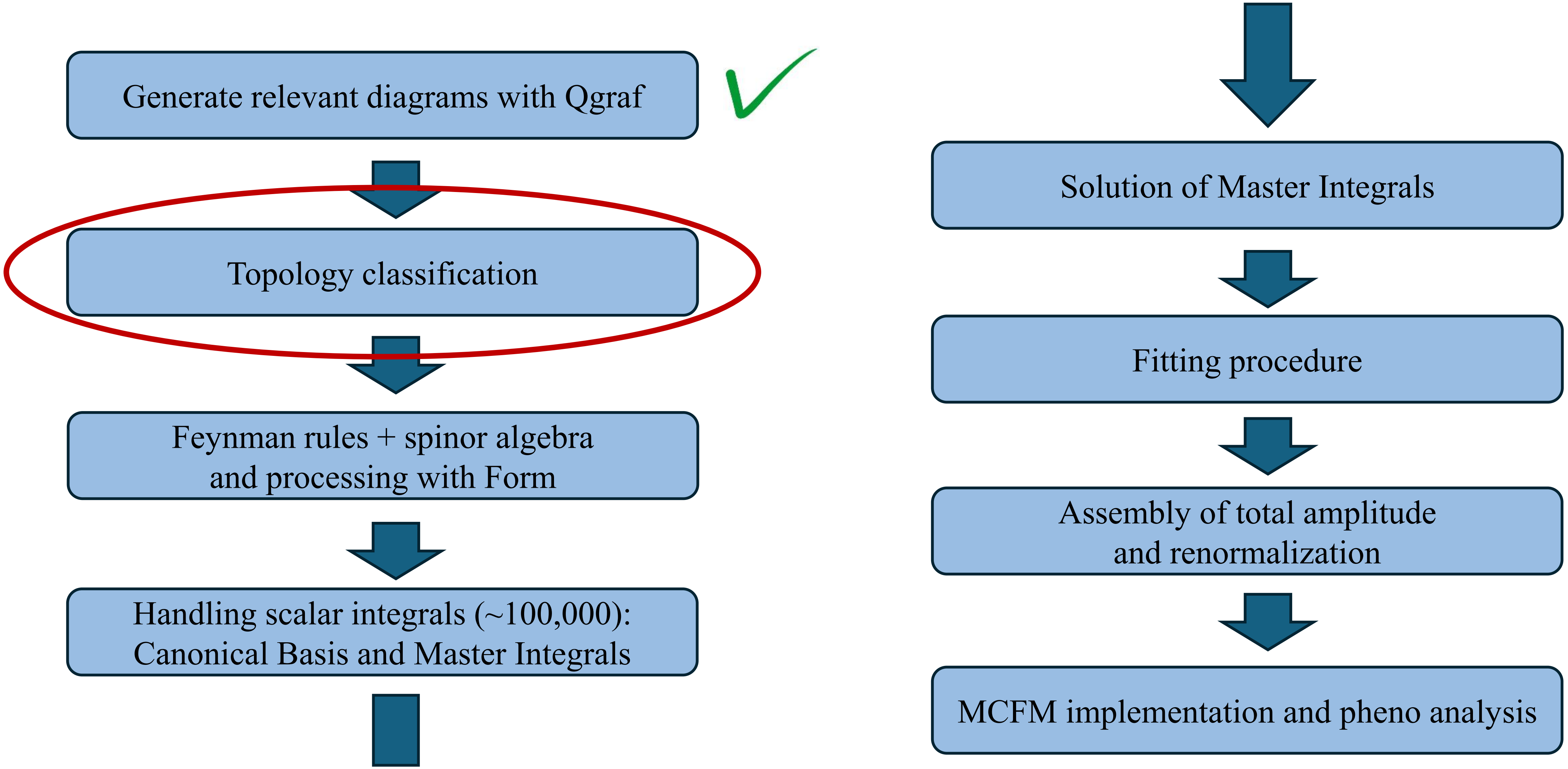

Topology Classification

- We identify 5 topologies:
  3 planar (P_I, P_{II}, P_{III}).
  2 non-planar (N_I, N_{II}).
- Topology P_{II} is technically a subtopology of P_{III} but it's convenient to separate them.
- Z-box type diagrams are expressed in terms of topology P_I.
- QED type diagrams are analyzed separately.

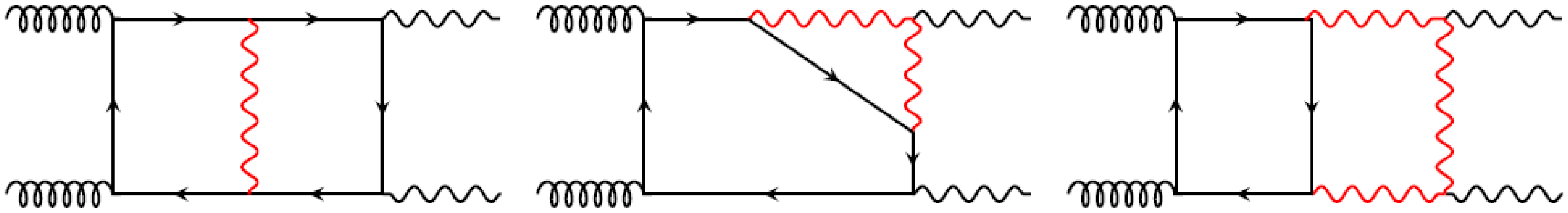

(a) Topology P_I (b) Topology P_{II} (c) Topology P_{III}

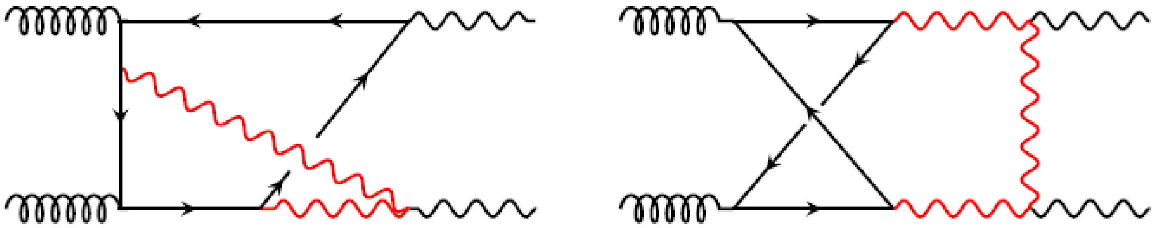

(d) Topology N_I (e) Topology N_{II}

Calculation Workflow

- Generate relevant diagrams with Qgraf ✓
- Topology classification ✓
- Feynman rules + spinor algebra and processing with Form
- Handling scalar integrals (~100,000): Canonical Basis and Master Integrals
- Solution of Master Integrals
- Fitting procedure
- Assembly of total amplitude and renormalization
- MCFM implementation and pheno analysis

Helicity Amplitudes: Tensor Structures

- The idea is to facilitate the calculation by using the well-known spinor-helicity formalism. → $$\mathcal{A}_{gg\to\gamma\gamma} = \varepsilon_\mu \varepsilon_\nu \varepsilon_\rho \varepsilon_\sigma \mathcal{A}^{\mu\nu\rho\sigma}_{gg\to\gamma\gamma}$$

- We write the amplitude in terms of a rank-4 Lorentz tensor, and we expand it into a tensor structure basis. → $$\mathcal{A}^{\mu\nu\rho\sigma}_{gg\to\gamma\gamma} = \sum_{i=1}^{N_T} \mathcal{F}_i \, T_i^{\mu\nu\rho\sigma}$$

- We construct Projectors based on those tensor structures and we extract the relevant form factors. → $$\mathcal{F}_{\lambda_i} = \sum_{pol} \mathcal{P}^{\mu\nu\rho\sigma}_{\lambda_i} \left(\varepsilon_{1,\mu}\right)^* \left(\varepsilon_{2,\nu}\right)^* \left(\varepsilon_{3,\rho}\right)^* \left(\varepsilon_{4,\sigma}\right)^* \mathcal{A}_{\lambda_1}$$

Physical Helicity Amplitudes

- From the Form Factors we can finally reconstruct the physical helicity amplitudes. We show one for brevity:

$$\mathrm{A}_{\lambda_1} = \frac{t^2}{4}\left(\frac{2\mathcal{F}_6}{u} - \frac{2\mathcal{F}_3}{s} - \mathcal{F}_1\right) + \mathcal{F}_8\left(\frac{s}{u} + \frac{u}{s} + 4\right) + \frac{t}{2}\left(\mathcal{F}_2 - \mathcal{F}_4 + \mathcal{F}_5 - \mathcal{F}_7\right)$$

- We have 8 independent helicity amplitudes. One for each of the following helicity configuration:

$$\begin{aligned} \lambda_1 &= \{+,+,+,+\}, & \lambda_2 &= \{-,+,+,+\} \\ \lambda_3 &= \{+,-,+,+\}, & \lambda_4 &= \{+,+,-,+\} \\ \lambda_5 &= \{+,+,+,-\}, & \lambda_6 &= \{-,-,+,+\} \\ \lambda_7 &= \{-,+,-,+\}, & \lambda_8 &= \{+,-,-,+\} \end{aligned}$$

- The form factors contain thousands of loop integrals → MIs reduction!

Calculation Workflow

Generate relevant diagrams with Qgraf ✓

Topology classification ✓

Feynman rules + spinor algebra
and processing with Form ✓

Handling scalar integrals (~100,000):
Canonical Basis and Master Integrals

Solution of Master Integrals

Fitting procedure

Assembly of total amplitude
and renormalization

MCFM implementation and pheno analysis

Auxiliary Topology

- We introduce an auxiliary topology to account for all the possible scalar products involving the loop momenta.

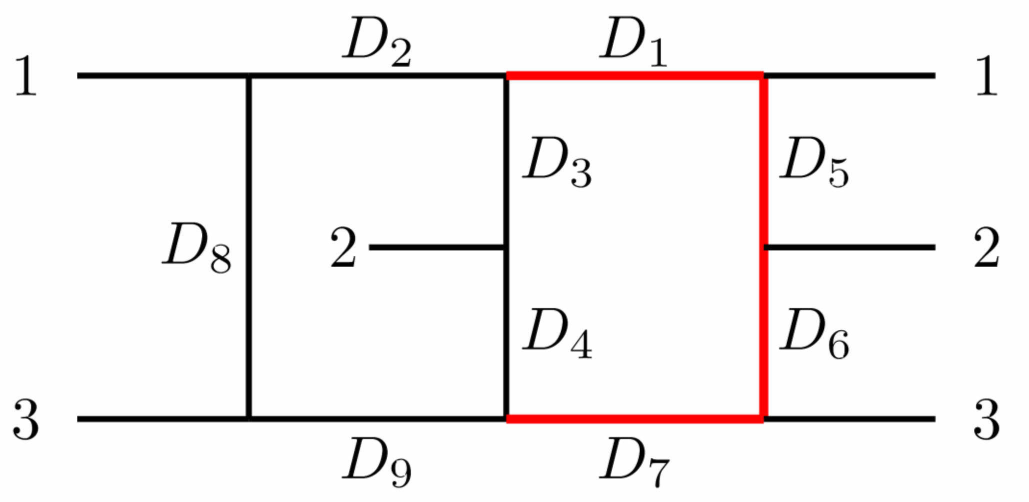

- All the scalar integrals can be written in terms of the auxiliary topology's propagators.

$$I^{\mathrm{N_{II}}}_{a_1\ldots a_9} = \mathcal{C}(\epsilon)\int \frac{d^d\ell_1}{(2\pi)^d}\frac{d^d\ell_2}{(2\pi)^d}\frac{1}{D_1^{a_1}\ldots D_9^{a_9}}$$

- This preliminary scalar integral reduction produces a multitude (~100,000) of scalar integrals! → Master Integral reduction

DEQ: Overview

- General strategy to evaluate MIs: Differential Equation method (DEQ)

Laporta Basis $\vec{\mathcal{I}}(\{x_i\})$ → $$\frac{\partial}{\partial x_i}\vec{\mathcal{I}}(\{x_i\}) = \underbrace{\mathcal{A}(\{x_i\},\epsilon)}\,\vec{\mathcal{I}}(\{x_i\})$$

- The complexity goes up pretty quickly for the Laporta Basis. Solution: Canonical Basis.

Canonical Basis $\vec{\mathcal{G}}(\{x_i\})$ → $$\frac{\partial}{\partial x_i}\vec{\mathcal{G}}(\{x_i\}) = \underbrace{\epsilon\mathcal{A}(\{x_i\})}\,\vec{\mathcal{G}}(\{x_i\})$$

- The factorization of the space-time parameter allows to write the solution in an iterative way:

$$\vec{\mathcal{G}}(\{x_i\}) = \left(\mathbb{1} + \epsilon\int_\gamma d\mathcal{A} + \epsilon^2\int_\gamma d\mathcal{A}\,d\mathcal{A} + \dots\right)\vec{\mathcal{G}}(\{x_i^0\})$$

DEQ: Canonical Basis

- The kinematic information is encoded in the alphabet $\{\eta_k\}$ of the differential equation:

$$d\mathcal{A} = \sum_k \mathcal{M}_k d\log\eta_k$$

- The solution for rational letters is expressed in terms of Goncharov Polylogarithms (GPLs) (*Goncharov, 1998*).

$$G(a_n,\ldots,a_1;x_0) = \int_0^{x_0} G(a_{n-1},\ldots,a_1;x_0)\frac{dt}{t-a_n}$$

- Efficient numerical evaluation of GPLs using GiNaC(*Vollinga, 2005*)/HandyG(*Naterop, Signer, Ulrich, 2016*).

- Non-rational letters may or may not be represented in terms of GPLs. We implement a generalized approach based on Chen's Iterated Integrals.

DEQ: Solution

In a more general scenario, the solution can be evaluated (up to boundary constants) at any fixed order:

$$\vec{\mathcal{G}}^{(1)}(\{x_i\}) = \int_\gamma d\mathcal{A}\,\vec{\mathcal{G}}^{(0)}(\{x_i^0\}) + \vec{\mathcal{G}}^{(1)}(\{x_i^0\})$$

$$\vec{\mathcal{G}}^{(2)}(\{x_i\}) = \int_\gamma d\mathcal{A}\,d\mathcal{A}\,\vec{\mathcal{G}}^{(0)}(\{x_i^0\}) + \int_\gamma d\mathcal{A}\,\vec{\mathcal{G}}^{(1)}(\{x_i^0\}) + \vec{\mathcal{G}}^{(2)}(\{x_i^0\})$$

$$\vec{\mathcal{G}}^{(3)}(\{x_i\}) = \int_\gamma d\mathcal{A}\,d\mathcal{A}\,d\mathcal{A}\,\vec{\mathcal{G}}^{(0)}(\{x_i^0\}) + \int_\gamma d\mathcal{A}\,d\mathcal{A}\,\vec{\mathcal{G}}^{(1)}(\{x_i^0\}) + \int_\gamma d\mathcal{A}\,\vec{\mathcal{G}}^{(2)}(\{x_i^0\}) + \vec{\mathcal{G}}^{(3)}(\{x_i^0\})$$

$$\begin{aligned}\vec{\mathcal{G}}^{(4)}(\{x_i\}) = &\int_\gamma d\mathcal{A}\,d\mathcal{A}\,d\mathcal{A}\,d\mathcal{A}\,\vec{\mathcal{G}}^{(0)}(\{x_i^0\}) + \int_\gamma d\mathcal{A}\,d\mathcal{A}\,d\mathcal{A}\,\vec{\mathcal{G}}^{(1)}(\{x_i^0\}) + \int_\gamma d\mathcal{A}\,d\mathcal{A}\,\vec{\mathcal{G}}^{(2)}(\{x_i^0\}) \\ &+ \int_\gamma d\mathcal{A}\,\vec{\mathcal{G}}^{(3)}(\{x_i^0\}) + \vec{\mathcal{G}}^{(4)}(\{x_i^0\}).\end{aligned}$$

Efficient semi-numerical implementation thanks to the recursive nature of the iterated integrals.

Calculation Workflow

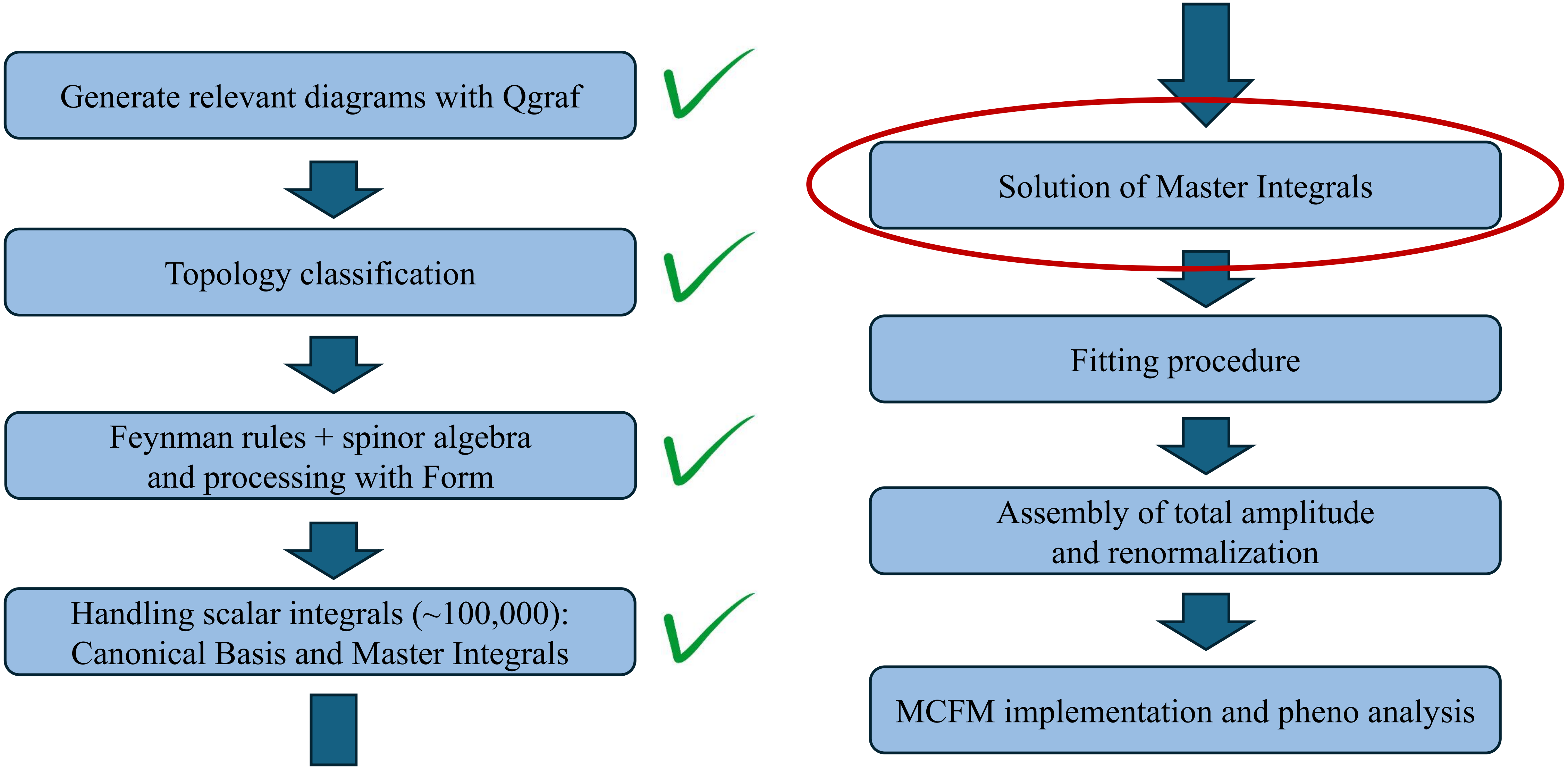

Rational vs Non-Rational alphabet

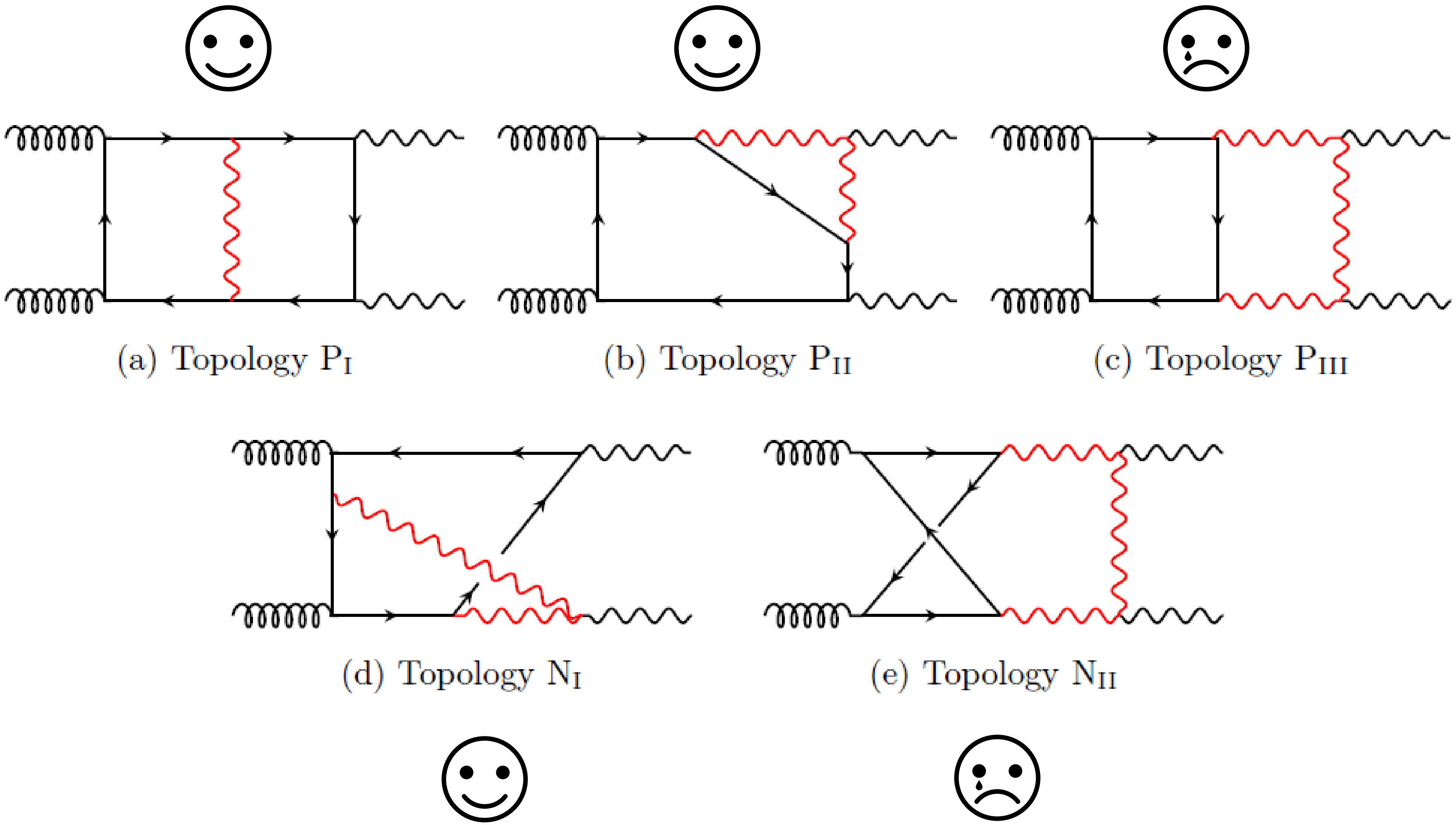

(a) Topology P_{I} (b) Topology P_{II} (c) Topology P_{III}

(d) Topology N_{I} (e) Topology N_{II}

The Canonical basis is obtained again via Magnus Series Expansion. Here we show the 7-propagators family:

$$
\begin{aligned}
\mathcal{G}_{29}^{\mathrm{P_{III}}} &= \epsilon^2 y \sqrt{r_2} \mathcal{F}_{29}, \\
\mathcal{G}_{30}^{\mathrm{P_{III}}} &= \epsilon^2 \sqrt{r_1} (2x\mathcal{F}_{28} + xy\mathcal{F}_{29} + y\mathcal{F}_{30}), \\
\mathcal{G}_{31}^{\mathrm{P_{III}}} &= \epsilon^2 y^2 (\mathcal{F}_{29} + \mathcal{F}_{31}), \\
\mathcal{G}_{32}^{\mathrm{P_{III}}} &= -\frac{1}{2}\epsilon \Big(2x(1-2\epsilon)\mathcal{F}_{21} + y^2\epsilon(-\mathcal{F}_{27} + x\mathcal{F}_{29} + \mathcal{F}_{30}) \\
&\quad + 2y\epsilon(2\mathcal{F}_{17} + \mathcal{F}_{22} + x\mathcal{F}_{28} + x\mathcal{F}_{29} - \mathcal{F}_{32}) \Big).
\end{aligned}
$$

The differential equation is expressed in terms of the variables:

$$
x = -\frac{2p_1 \cdot p_2}{M_W^2} \qquad y = -\frac{2p_2 \cdot p_3}{M_W^2}
$$

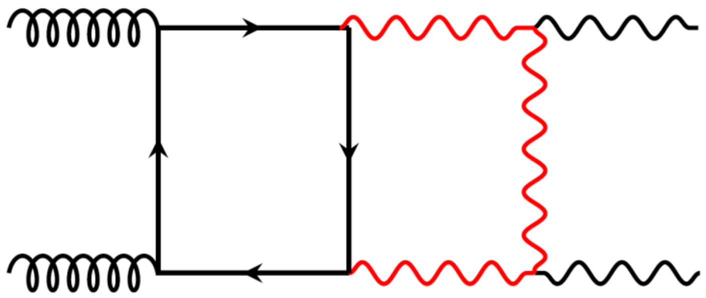

- Non-Rational letters:

$$
\begin{aligned}
r_1 &= y(4+y), \\
r_2 &= y\left(y + 2xy + x^2(4+y)\right), \\
r_3 &= xy\left(4y + x(4+y)\right).
\end{aligned}
$$

- For efficiency reasons, we only rationalize r_1.

Topology P_{III}: Kinematic Sub-Regions

$$\text{Region A}: [0 \geq y \geq -4, \;\; x \leq -y], \quad y = -\frac{4z_A^2}{1+z_A^2} \qquad \text{Region B}: [y \leq -4, \;\; x \leq -y], \quad y = -\frac{4}{1-z_B^2}$$

$$\mathcal{G}_i^{\mathrm{P_{III}}}(x=0)$$

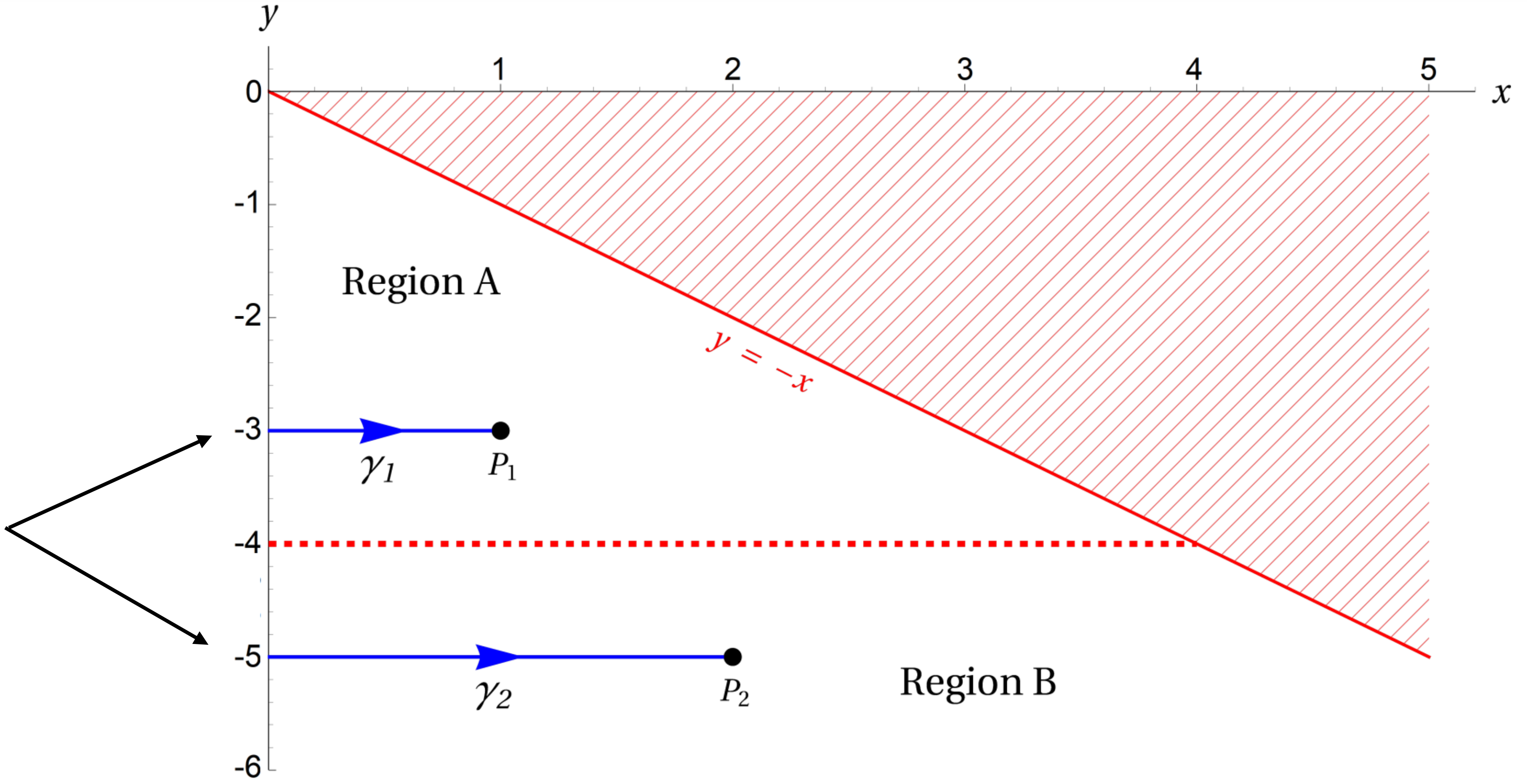

Topology P_{III}: Numerical Evaluation and AMFlow Check

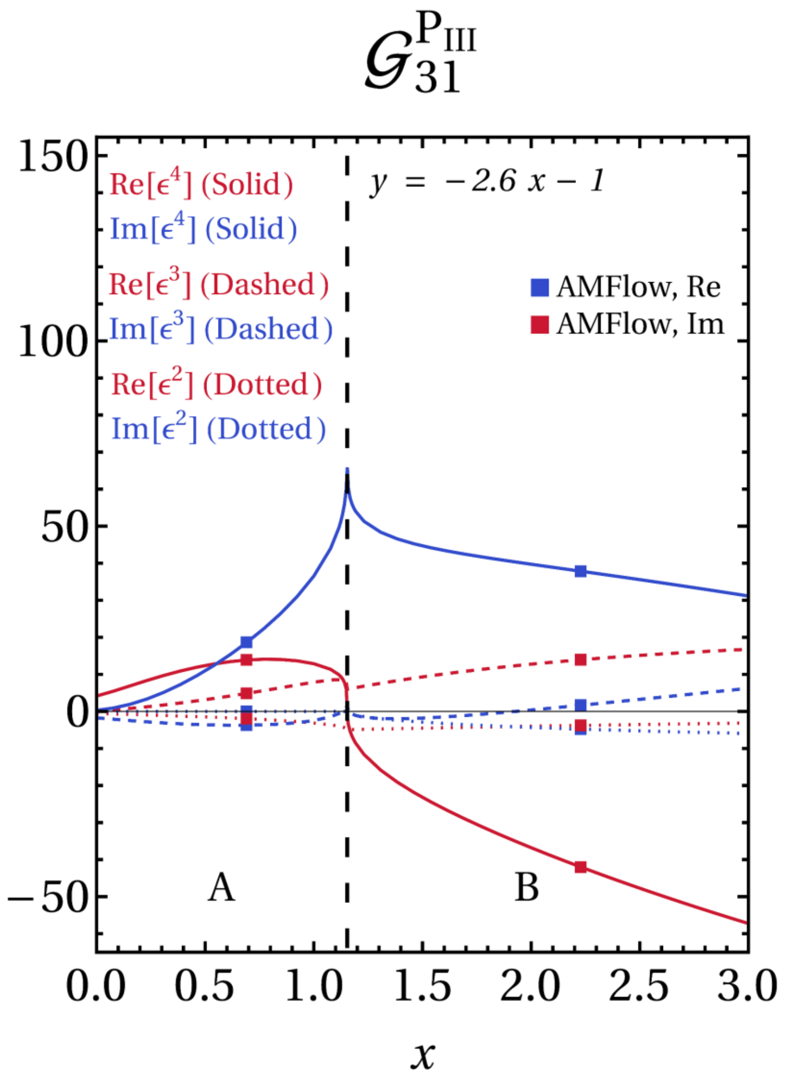

Integration Path:

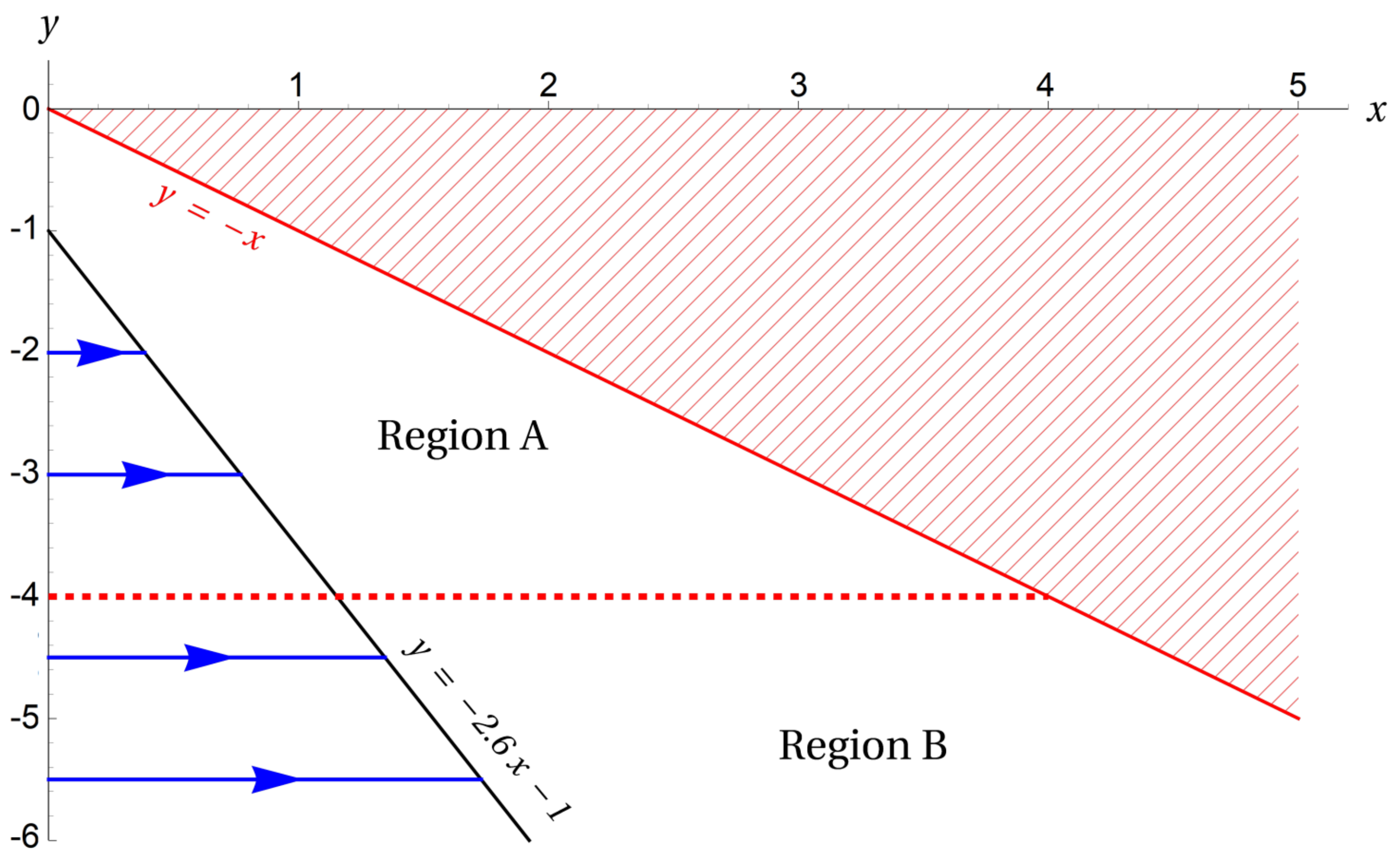

Calculation Workflow

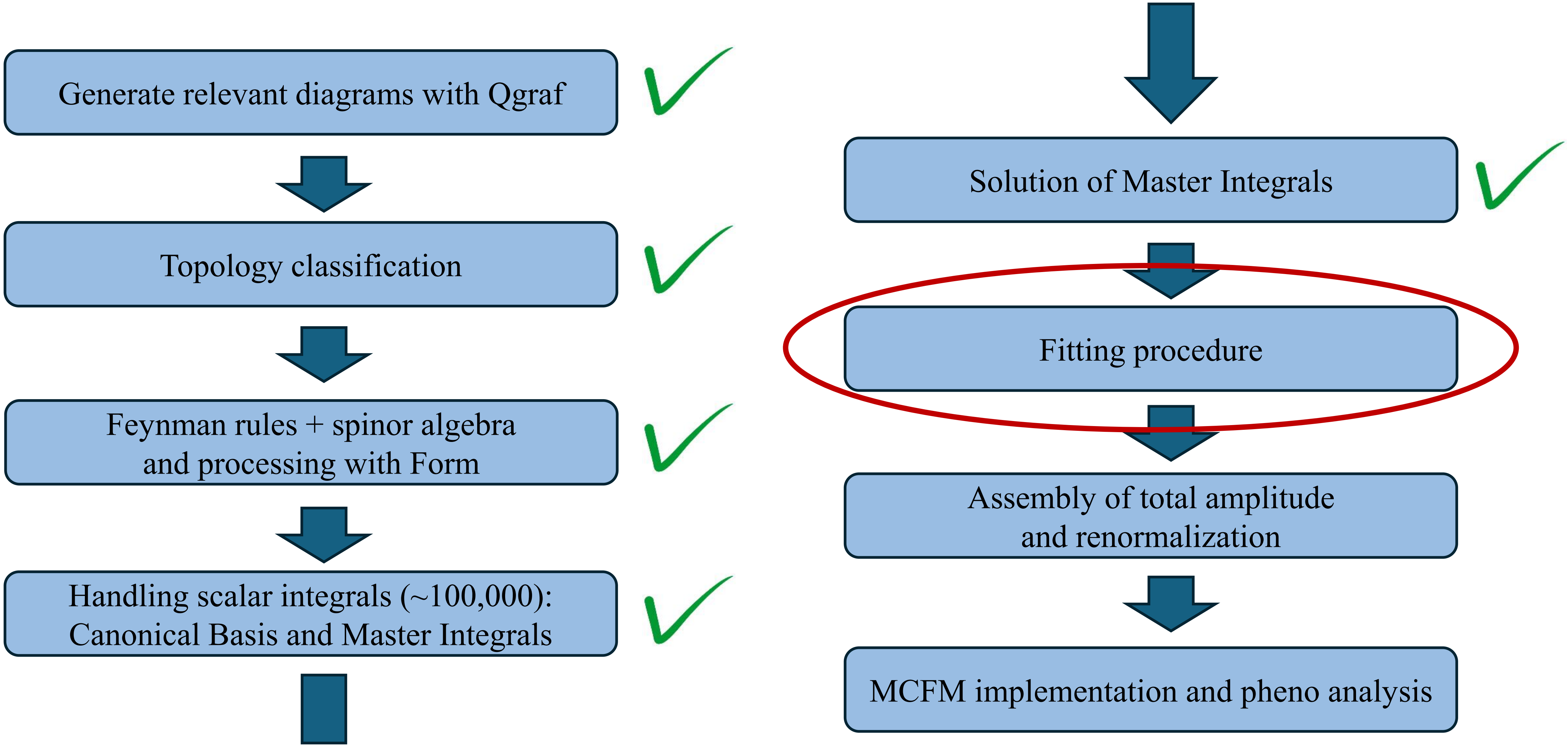

Fitting Procedure: Methodology

- Once we have the MIs we can evaluate them. GPL vs Chen.

- Overall goal: MCFM implementation. It is Crucial to find an efficient evaluation over the phase space.

- Idea: generate a grid of values in Mathematica and try a fitting strategy. Very efficient and reliable if successful, but control over the errors introduced by the approximation is mandatory.

- Exploit the underlying logarithmic structure of Chen Integrals. Fit real and Imaginary part separately:

$$\mathcal{K}_n^{(w)}(x,y) = \frac{\sum_{i+j=6} a_{i,j} x^i y^j}{\sum_{i+j=6} b_{i,j} x^i y^j} + i \frac{\sum_{i+j=6} c_{i,j} x^i y^j}{\sum_{i+j=6} d_{i,j} x^i y^j}$$

Fitting Procedure: Regions

- To prevent numerical instabilities given by real and pseudo thresholds, it's more efficient do break down the fitting by regions.

Topology P_{III}

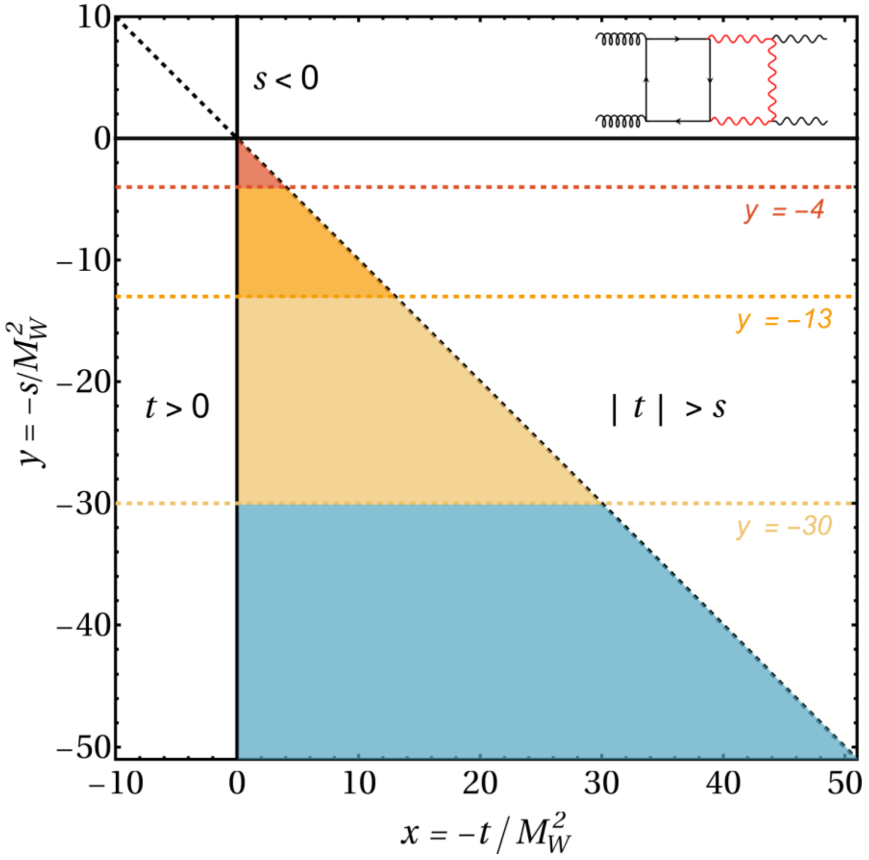

Topology N_{II}

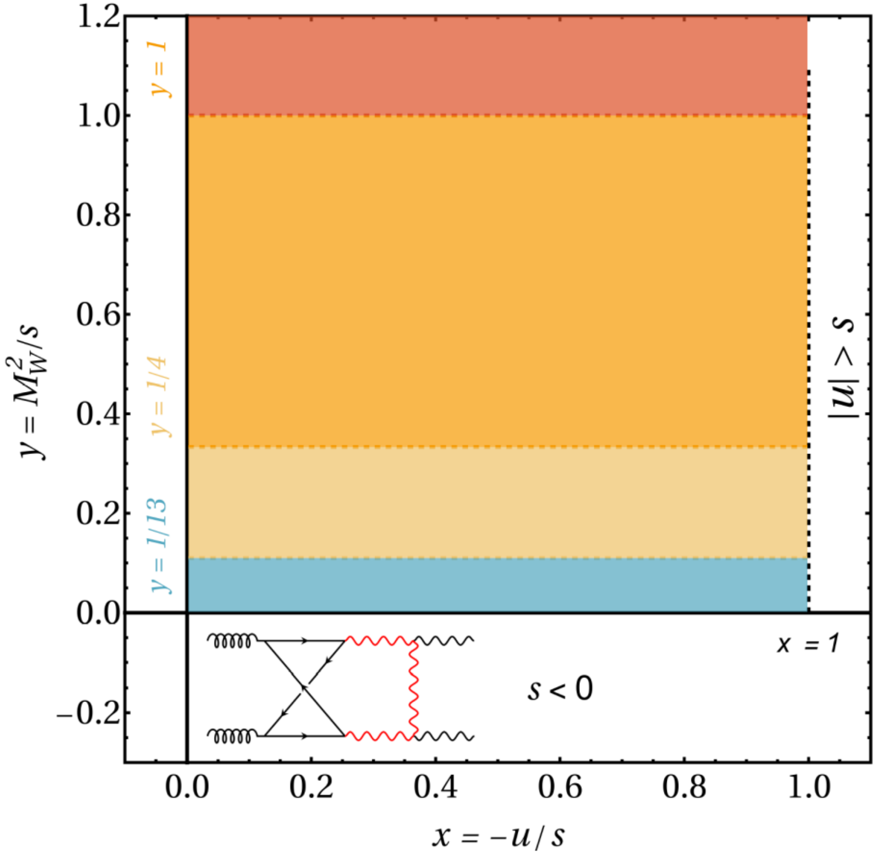

Fitting Procedure: Validation

- Preliminary analysis shows very good accuracy across the phase-space. Do the pseudo-thresholds cause any real issue? We find an estimate on the cross-section for the fully integrated effects!

- Idea: use NI as a tetsing ground. Most complex GPL topology ~ 20,000 GPL!

- We compare analytic $\sigma_{\mathrm{N_I}}^{(\mathcal{G})}$ vs fitting $\sigma_{\mathrm{N_I}}^{(\mathcal{K})}$ and extract a comparison from there. Expect similar behaviour from PIII and NII.

Ratio $\sigma_{\mathbf{N_I}}^{(\mathcal{K})}/\sigma_{\mathbf{N_I}}^{(\mathcal{G})}$	**Uncertainty**
1.00001	± 0.007

Calculation Workflow

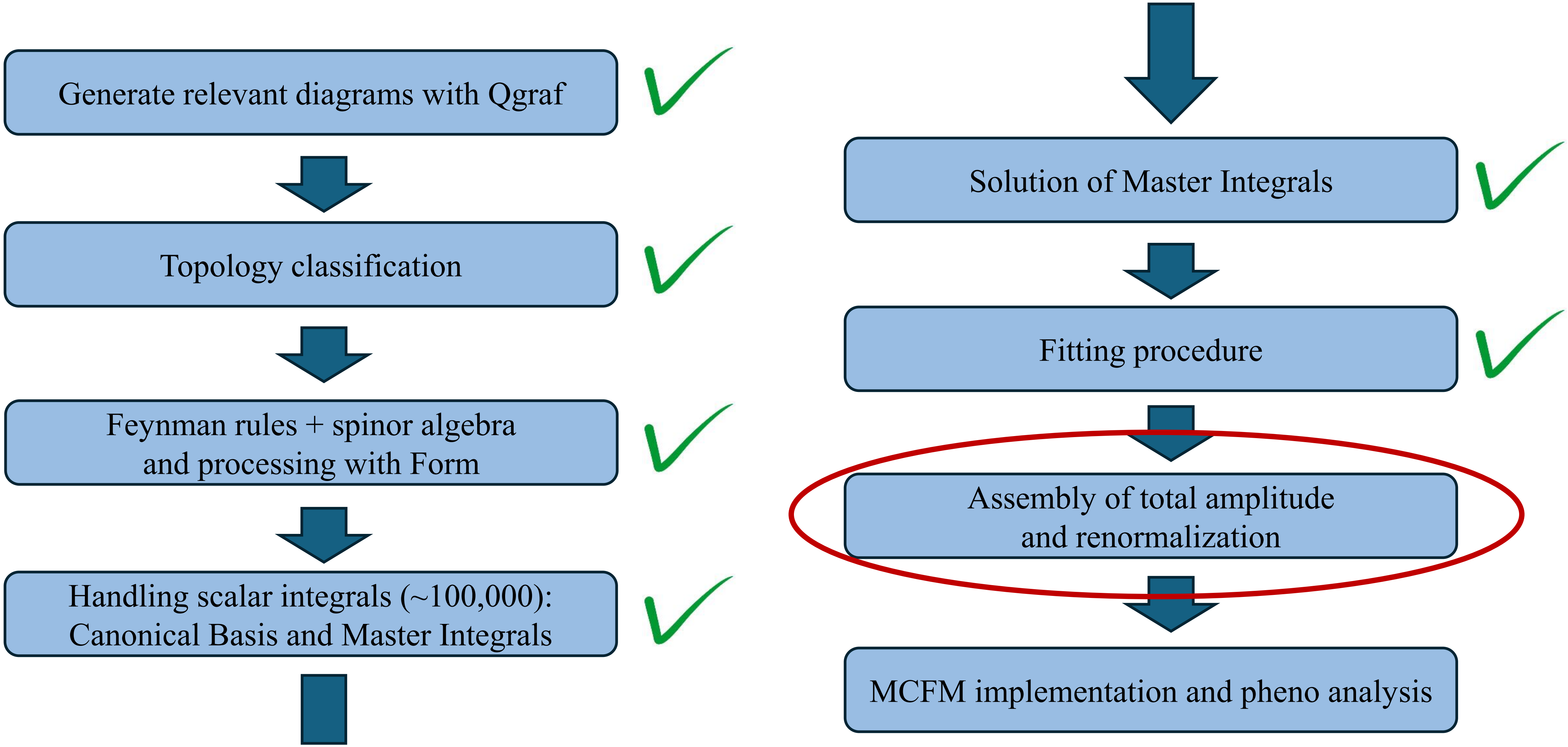

Various validations for our results:

- Extensive numerical check for MIs with AMFlow.
- IR and UV analytic cancellation.
- Comparison for LO and NLO QED corrections with the literature.
- Scheme independence for γ_5.
- Invariance under $u \leftrightarrow t$ and symmetry of rapidity distribution.

Calculation Workflow

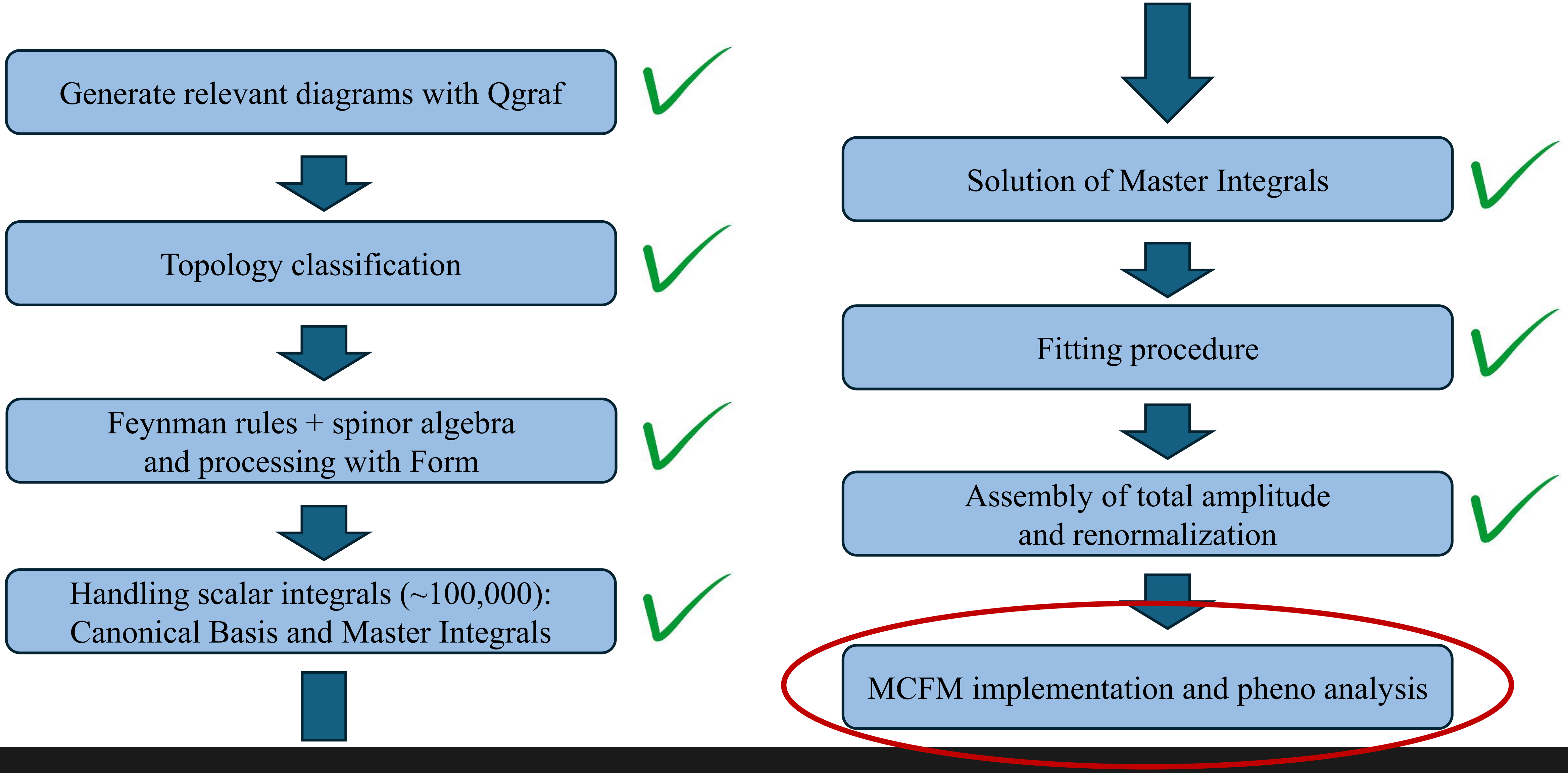

MCFM Setup

- We present the results of our implementation for:

    1) Total cross-section,
    2) Invariant mass $m_{\gamma\gamma}$ distribution,
    3) Transverse momentum p_T distribution,
    4) Rapidity of the system $Y_{\gamma\gamma}$ distribution.

- It's phenomenologically interesting to distinguish between two different invariant mass regions:

"Higgs" window

$$M_Z < m_{\gamma\gamma} < 2M_W$$

"High-energy" window

$$2M_W < m_{\gamma\gamma} < 500 GeV$$

Results: Cross-section

Correction of ~ 2.43% in the Higgs window

Order	Cross Section [pb]	Uncertainty [pb]
$\tilde{\sigma}^{(\mathrm{LO})}_{gg\to\gamma\gamma}$	2.176	$\pm\,0.002$
$\tilde{\sigma}^{(\mathrm{NLO\text{-}EW})}_{gg\to\gamma\gamma}$	2.229	$\pm\,0.003$

Correction of ~ 1.62% in the high energy region

Order	Cross Section [pb]	Uncertainty [pb]
$\tilde{\sigma}^{(\mathrm{LO})}_{gg\to\gamma\gamma}$	0.39119	$\pm\,0.00001$
$\tilde{\sigma}^{(\mathrm{NLO\text{-}EW})}_{gg\to\gamma\gamma}$	0.39751	$\pm\,0.00006$

Results: Invariant Mass Distributions

"Higgs" window | **"High-energy" window**

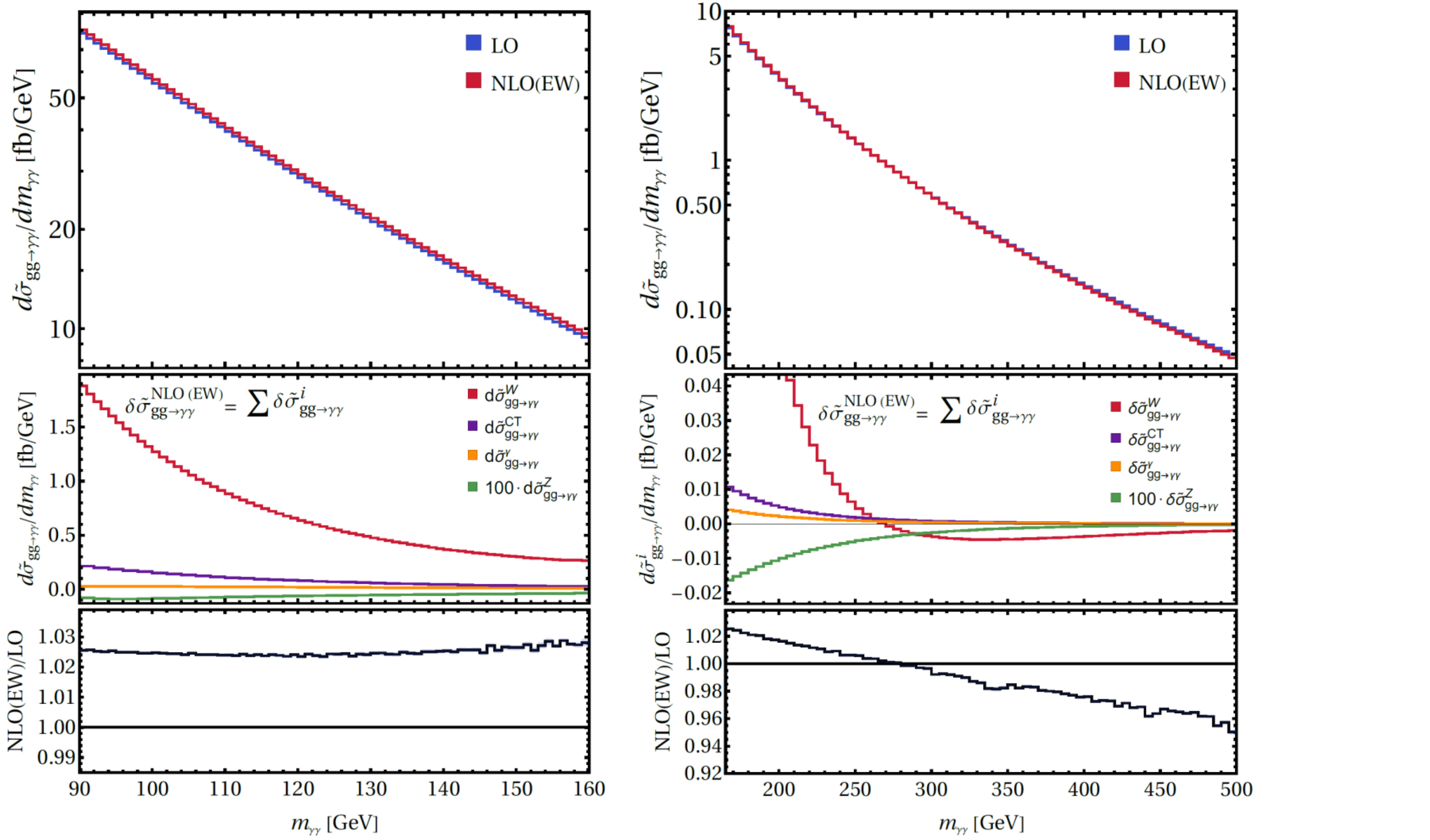

Results: Transverse Momentum Distributions

“Higgs” window

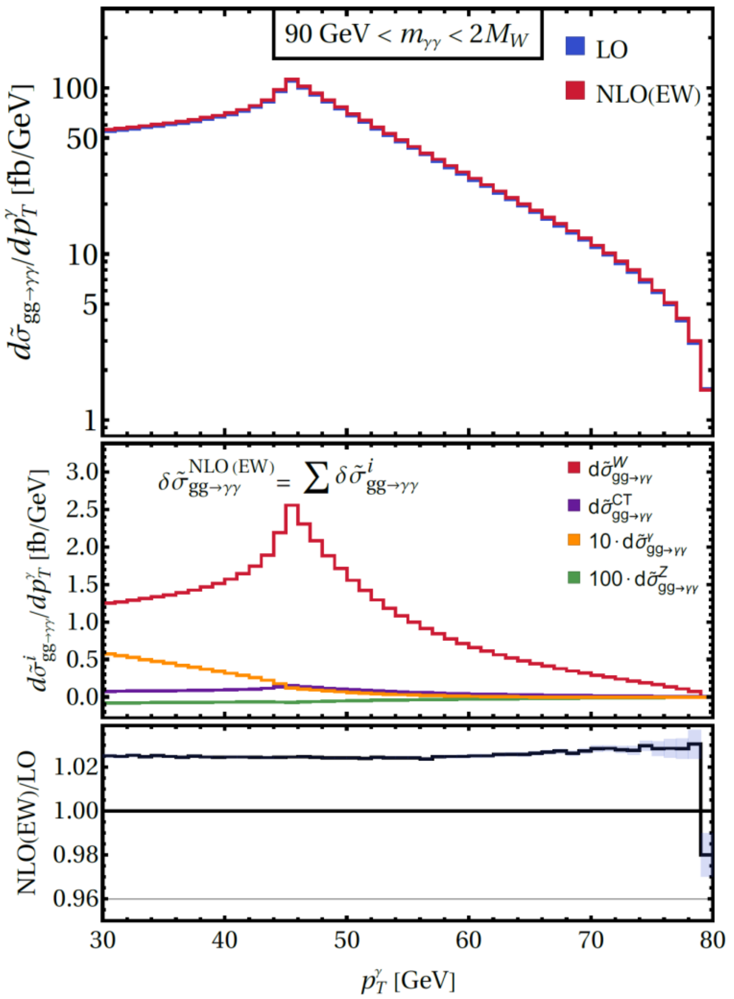

“High-energy” window

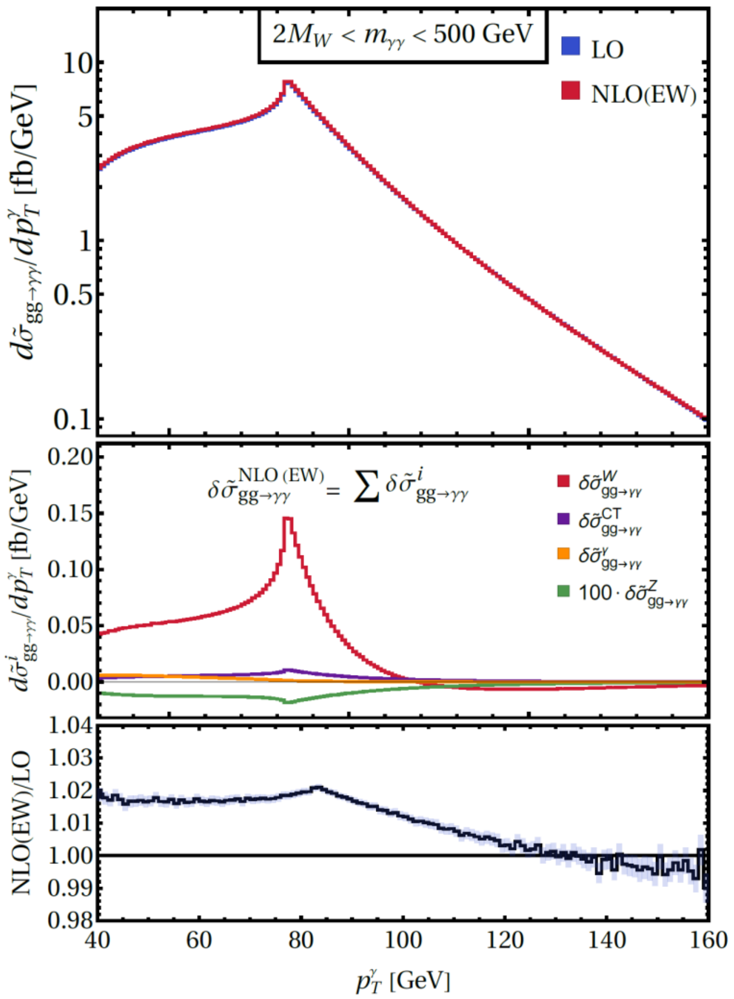

Results: Rapidity Distributions

"Higgs" window

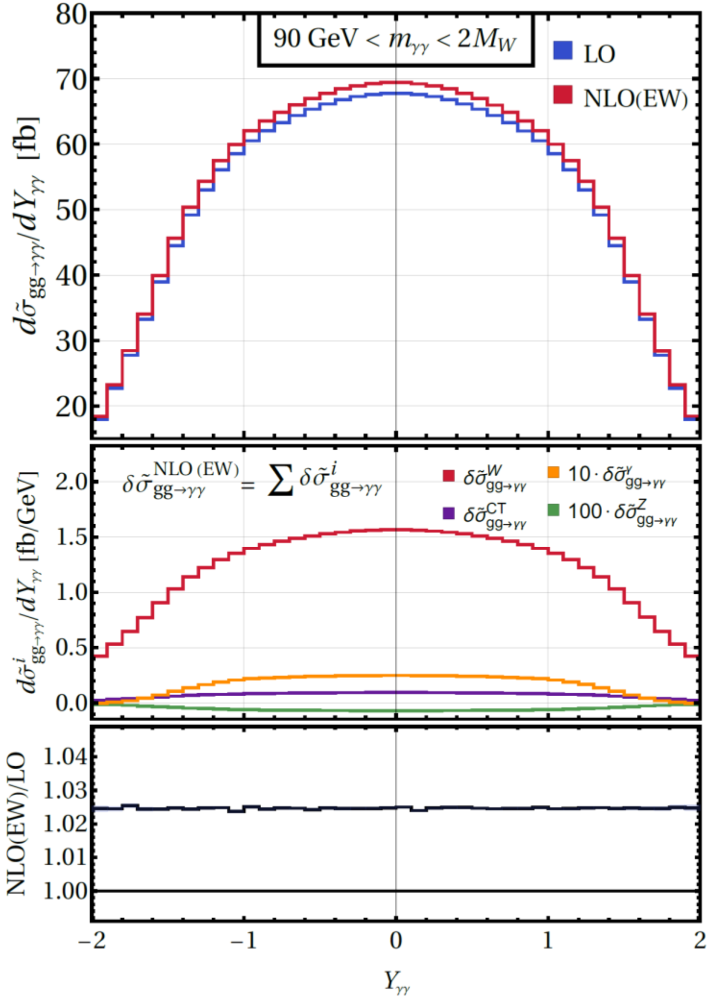

"High-energy" window

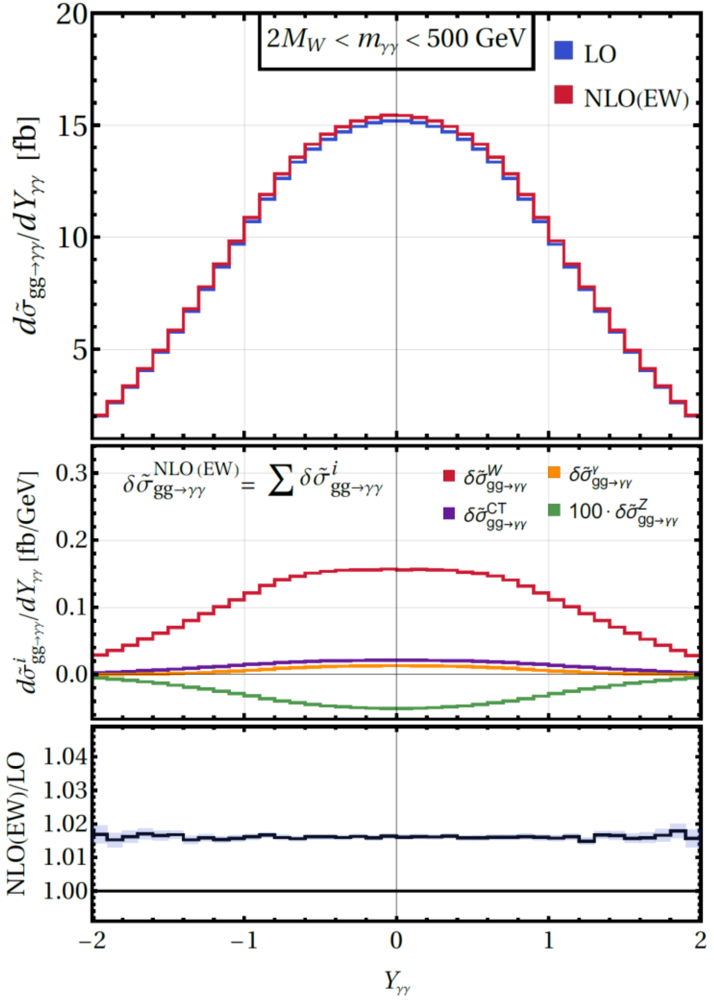

Summary and Future Plans

- Evaluation for the first time of EW correction to $gg \to \gamma\gamma$ for light quarks. We observed impact of 2.43% in the Higgs central region, and a more modest impact of 1.62% in the high energy region.

- Differential distributions shows corrections at the percent level, with more structure happening in the high energy region. Symmetry of the rapidity distribution contitues a non-trivial check for our results.

- We expect the high energy region to be sensitive to the top-quark correction ⟹ Work in progress!

- With the inclusion of the top-quark corrections, we can calculate the EW correction to the Higgs interference and ultimately extrapolate the corresponding corrections to the Higgs Width

Thank you for listening!